Title
Energetically significant networks of coupled interactions within an unfolded protein

Journal
Proceedings of the National Academy of Sciences of the United States of America, 111(33)

ISSN
0027-8424

Authors
Cho, Jae-Hyun
Meng, Wenli
Sato, Satoshi
et al.

Publication Date
2014-08-19

DOI
10.1073/pnas.1402054111

Peer reviewed

Energetically significant networks of coupled interactions within an unfolded protein

Jae-Hyun Cho[a,1], Wenli Meng[b,1], Satoshi Sato[b], Eun Young Kim[c], Hermann Schindelin[d], and Daniel P. Raleigh[b,2]

[a]Department of Biochemistry and Biophysics, Texas A&M University, College Station, TX 77843-2128; [b]Department of Chemistry, Stony Brook University, Stony Brook, NY 11794; [c]Department of Biochemistry, Center for Structural Biology, Stony Brook University, Stony Brook, NY 11794; and [d]Rudolf Virchow Center for Experimental Biomedicine and Institute of Structural Biology, University of Würzburg, 97080 Würzburg, Germany

Edited by Robert L. Baldwin, Stanford University, Stanford, CA, and approved June 24, 2014 (received for review February 4, 2014)

Unfolded and partially unfolded proteins participate in a wide range of biological processes from pathological aggregation to the regulation of normal cellular activity. Unfolded states can be populated under strongly denaturing conditions, but the ensemble which is relevant for folding, stability, and aggregation is that populated under physiological conditions. Characterization of nonnative states is critical for the understanding of these processes, yet comparatively little is known about their energetics and their structural propensities under native conditions. The standard view is that energetically significant coupled interactions involving multiple residues are generally not present in the denatured state ensemble (DSE) or in intrinsically disordered proteins. Using the N-terminal domain of the ribosomal protein L9, a small α-β protein, as an experimental model system, we demonstrate that networks of energetically significant, coupled interactions can form in the DSE of globular proteins, and can involve residues that are distant in sequence and spatially well separated in the native structure. X-ray crystallography, NMR, dynamics studies, native state pK_a measurements, and thermodynamic analysis of more than 25 mutants demonstrate that residues are energetically coupled in the DSE. Altering these interactions by mutation affects the stability of the domain. Mutations that alter the energetics of the DSE can impact the analysis of cooperativity and folding, and may play a role in determining the propensity to aggregate.

protein folding | protein stability | ϕ-value analysis | double-mutant cycle

The properties of nonnative states of proteins have attracted considerable attention because they can play critical roles in cell signaling, translocation across membranes, temperature-sensitive phenotypes, and in a wide range of protein deposition diseases (1–14). The properties of unfolded states are also relevant to any discussion of intrinsically disordered proteins (IDPs) (1). The denatured state ensemble (DSE) can be populated under strongly denaturing conditions and studied at equilibrium; however, the physiologically relevant DSE is the state that is in equilibrium with the folded state under native conditions. This state is difficult to study directly and most studies of the DSE under native conditions have made use of indirect approaches. Nevertheless, experimental and theoretical work has shown that the DSE populated under physiological conditions is not a random coil, but can contain native and nonnative structure, stabilized by local and nonlocal interactions. However, very little is known about the energetics of these interactions, particularly ones involving residues distant in sequence, or about energetically coupled interactions involving multiple residues in the DSE (15–19). These are a critical piece of the folding puzzle; they impact protein aggregation and folding, and have important implications for the properties of IDPs. Recent studies offer evidence for hydrophobic clusters, electrostatic interactions, and residual secondary structure in the DSE under near-native conditions (20–22). This naturally leads to the questions of how DSE interactions contribute to protein stability and folding, and if networks of coupled interactions occur in the DSE. The energetics of DSE interactions are not nearly as well understood as native state interactions, and the possibility of networks of interactions in the DSE are generally not considered. Such effects, were they to exist, could have a significant impact on protein stability, on the analysis of cooperative interactions, and on protein folding. They could also impact the propensity of proteins to aggregate.

Here we show that energetically significant nonnative and native interactions, involving multiple residues that are distant in the primary sequence and spatially well resolved in the native structure, can form in the DSE of globular proteins. The interactions include hydrophobic clusters as well as electrostatic interactions and are coupled in the sense that perturbing one interaction modulates others. Altering these interactions by mutation affects protein stability and can complicate the analysis of the coupling in the native state and folding, if they are not accounted for.

Results and Discussion

The N-terminal domain of the ribosomal protein L9 (NTL9) is used as a model system for these studies. It adopts a common α-β structure, folds in an apparent two-state manner as judged by extensive equilibrium and kinetic studies (Fig. 1*A*) (21, 23–26). Of particular interest is the observation of nonnative interactions in the DSE of NTL9 involving K12 (21, 24). Replacement of K12 by Met increases the stability of the domain by 1.9 kcal mol^{-1}, a result which is thought to be dominated by DSE effects (21, 24). Significant interactions have been observed in the DSE of

Significance

Unfolded and partially unfolded proteins participate in a wide range of biological processes from pathological aggregation to the regulation of normal cellular activity. Characterization of nonnative states is critical for the understanding of these processes, yet comparatively little is known about their energetics and their structural propensities under native conditions. We demonstrate that energetically important interactions, which involve multiple residues and which include significant nonnative effects, can form in the denatured state ensemble (DSE) of globular proteins, and can involve residues that are distant in sequence and spatially well separated in the native structure. Mutations that alter the energetics of the DSE can impact the analysis of cooperativity and folding, and could modulate the propensity to aggregate.

Author contributions: J.-H.C., W.M., and D.P.R. designed research; J.-H.C., W.M., and S.S. performed research; S.S. and E.Y.K. contributed new reagents/analytic tools; J.-H.C., W.M., H.S., and D.P.R. analyzed data; and J.-H.C., W.M., H.S., and D.P.R. wrote the paper.

The authors declare no conflict of interest.

This article is a PNAS Direct Submission.

Data deposition: The atomic coordinates and structure factors have been deposited in the Protein Data Bank, www.pdb.org [PDB ID codes 2HBB (NTL9 wild type) and 2HBA (K12M NTL9)].

[1]J.-H.C. and W.M. contributed equally to this work.

[2]To whom correspondence may be addressed. Email: daniel.raleigh@stonybrook.edu.

This article contains supporting information online at www.pnas.org/lookup/suppl/doi:10.1073/pnas.1402054111/-/DCSupplemental.

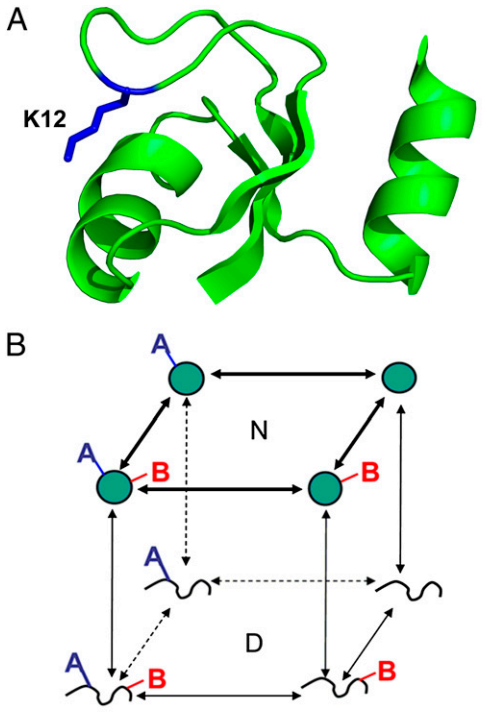

Fig. 1. (*A*) Ribbon diagram of the NTL9 (PDB ID code 2HBB). The N terminus is labeled and the side chain of K12 is shown in stick format. (*B*) Thermodynamic cycle analysis. The upper side of the cube represents a double-mutant cycle in the native state and the bottom side represents a double-mutant cycle in the DSE. N and D represent, respectively, the native state and the DSE. Two residues, A and B, can be thermodynamically linked through either the native state or the DSE or both. ΔG°_{EAB}, ΔG°_{EA}, ΔG°_{EB}, and ΔG°_{E} represent the unfolding free energies of wild type, a single mutant at site B, a single mutant at site A, and the double mutant, respectively. A negative coupling free energy represents either an unfavorable interaction in the native state or a favorable interaction in the DSE or a combination of both. A negative value will also arise if a favorable DSE interaction is larger than a favorable native state interaction and vice versa.

other proteins, thus NTL9 is not an isolated example (4, 10, 14, 18, 22, 27).

Thermodynamic Analysis Reveals that K12 is Coupled to an Extensive Set of Hydrophobic Residues in the Denatured State Ensemble. We used standard double-mutant cyclic analysis to measure the apparent thermodynamic coupling between K12 and 15 different core residues to test for the presence of energetically significant interactions (Figs. 1*B* and 2 *A*–*C* and Tables S1 and S2) (28). Double-mutant cycle analysis is the classic method to detect energetic coupling between residues; the observation that a double mutant has a larger effect on protein stability than expected from the sum of the effects of the two single mutants indicates an energetic coupling (29–31). The analysis is commonly described by a 2D cycle, a thermodynamic square, in which the free energy of the DSE is assumed not to be perturbed. A rigorous description requires a thermodynamic cube that includes potential DSE effects (Fig. 1*B*) (30, 32). The original work on double-mutant cycles carefully pointed out the necessity to consider the DSE, but DSE effects have often been ignored since then (31).

K12 is on the surface of the protein and its ε-amino group is completely exposed to solvent in the native state (Figs. 2*C* and 3*A*). The mutated sites are distributed widely throughout the native structure with distances to K12 ranging from 6.0 Å to 23.5 Å (Fig. 2 and Table S2). Two of the mutated residues (A22 and A42) are fully exposed to solvent. All of the mutants are folded and exhibit cooperative unfolding transitions. Surprisingly, the double-mutant cycle analysis showed that 14 out of 15 of these residues are strongly thermodynamically coupled with the ε-amino group of K12, despite the fact that none of them makes direct contact with K12 in the native state, and despite the fact that the ε-amino group in the K12 side chain is solvent exposed (Fig. 2). The average interaction free energy between K12 and these 14 residues is -0.97 ± 0.41 kcal mol^{-1} and there is no correlation between the distance from K12 in the native state and the interaction free energy (Fig. 2*B* and Table S2). The simplest interpretation of this data set is that the mutations alter DSE interactions, and that this contributes to the observed interaction free energies. Some of the effects likely include partial contributions from alteration of native state interactions, but the data presented below show that DSE effects play an important role.

The K12M Mutation Does Not Affect the Structure or Dynamics of the Native State of NTL9. Structural changes induced by mutation can propagate through the tightly packed hydrophobic core of proteins and can generate cooperative coupling between distant residues (33). However, the side chain of K12 is solvent exposed, and it is difficult to imagine how K12 could form a network involving 14 of 15 hydrophobic core residues, many of which are well separated from each other in the native structure. Our high-resolution crystal structures and NMR studies show that the K12M mutation does not alter the native state structure. We solved the structure of wild-type and K12M NTL9 at 1.9 Å and 1.25 Å resolution, respectively (Fig. 3*A* and Table S3). The two structures are virtually identical, with a backbone root-mean-square deviation of 0.70 Å for residues 1–51. The C-terminal five residues are partially flexible and are not well-defined in the

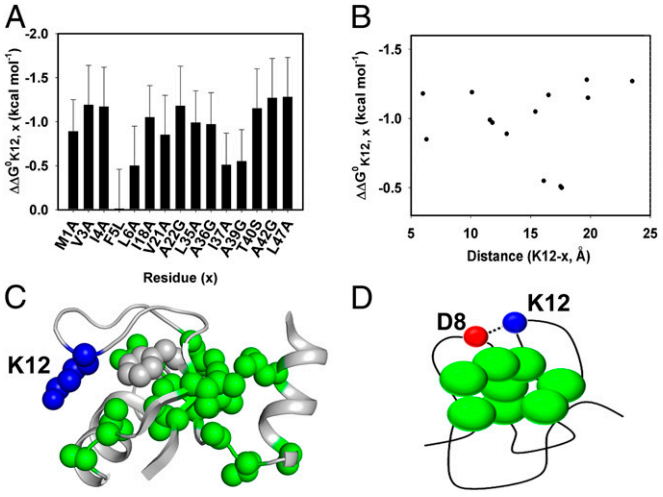

Fig. 2. K12 is energetically coupled to hydrophobic core residues. Measured thermodynamic interaction free energies ($\Delta\Delta G^{\circ}_{K12,X}$) between K12 and various hydrophobic residues. (*A*) Histogram of the $\Delta\Delta G^{\circ}_{K12,X}$ values. (*B*) Plot of the $\Delta\Delta G^{\circ}_{K12,X}$ values vs. the distance between K12 and the site of mutation in the native state (defined as the distance between the ε-amino group of K12 and the closest nonhydrogen atom of residue x). There is no correlation between the coupling free energy and distance. (*C*) Structure of NTL9. K12 is shown in stick format and the core residues are shown in space filling format. Residues which are apparently coupled to K12 are in green; the one which is not is in silver. (*D*) A cartoon depicting the potential origin of the coupling in the DSE. Transient hydrophobic clusters, residues depicted as circles, stabilize nonnative electrostatic interactions involving K12. Disruption of the hydrophobic clusters, for example by mutation of Leu to Ala, is predicted to weaken the coupling between K12 and other sites.

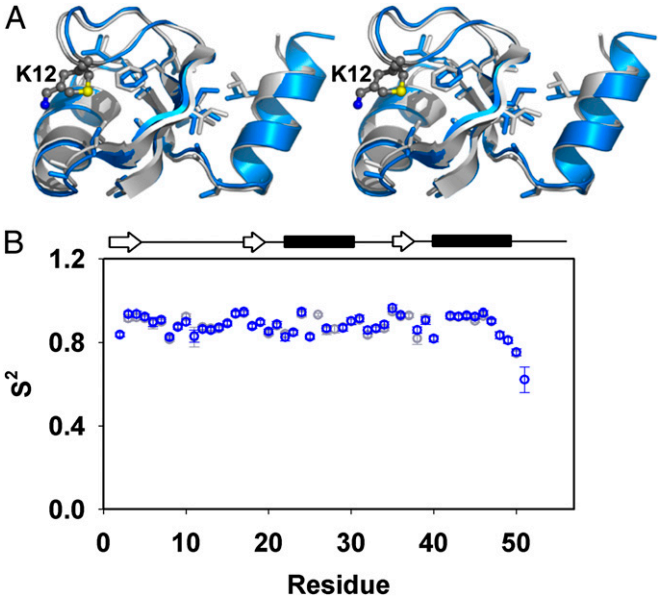

Fig. 3. The K12M mutation does not perturb the structure. (*A*) Stereoview of crystal structures of wild-type and the K12M mutant of NTL9. Superposition of the two structures with the wild type (PDB ID code 2HBB) in gray and the K12M variant (PDB ID code 2HBA) in blue. The side chain of residue 12 is shown in ball-and-stick representation, whereas hydrophobic side chains are shown in all-bonds representation. (*B*) ^{15}N order parameters for wild-type (gray) and K12M (blue) NTL9. Data are plotted as S^2 vs. residue number. A schematic diagram of the native state secondary structure is shown at the top of the plot. β-strands are depicted as arrows and α-helices as bars.

crystal structures, but have similar chemical shifts in their NMR spectra. The conformations of the residues in the hydrophobic cores of the wild-type and K12M mutant are identical with only one minor exception. The side chain of L47 is rotated about its $C_{\alpha\text{-}\beta}$ bond in the K12M mutant; however, this change is compensated by a rotation of the side chain of I4 about its $C_{\alpha\text{-}\beta}$ bond. The result is that these two residues still occupy the same relative position (Fig. S1).

NMR studies provide further evidence that the K12M mutation does not alter the structure. C_α proton chemical shifts are very sensitive to local changes in structure, whereas the temperature dependence of amide proton chemical shifts provides information about hydrogen bonding and protein dynamics which may not be probed in static crystal structures (34). The C_α proton chemical shifts and the temperature coefficients of the amide chemical shifts of wild type and K12M are virtually identical (21) (Fig. S2).

We next examined the effect of the K12 mutation on native state dynamics. Amide H/D exchange rates are sensitive to local and global fluctuations. Previously reported, NMR-detected, H/D exchange experiments conducted under EX2 conditions have shown that the identity of the residues that exchange by local unfolding and those which exchange by global unfolding are the same for wild-type and K12M NTL9, suggesting that the mutation does not perturb the pattern of local fluctuations (21). ^{15}N NMR relaxation studies provide a more direct probe of backbone dynamics. There are no changes in NMR-detected backbone dynamics in the K12M mutant compared with wild type. We measured ^{15}N order parameters for both wild-type NTL9 and the mutant, and the values are identical within the experimental uncertainty (Fig. 3*B*).

A further probe of the consequences of the K12 mutation is provided by native state pK_a measurements for the six acidic residues in wild-type NTL9 and in the K12M mutant. pK_a measurements report native state electrostatic energetics and are a sensitive probe of the effect of mutations (35). The pK_a values are identical in the two proteins, indicating that the mutation does not perturb native state electrostatic interactions involving the acidic side chains (Table S4) (21, 24).

Double-Mutant Cycle Analysis Reveals the Presence of Energetically Significant, Coupled Interactions in the Denatured State Ensemble. The thermodynamic studies indicate that K12 is coupled to a multitude of hydrophobic sites. A cartoon representative of how this might occur is depicted in Fig. 2*D*. We hypothesize that nonnative electrostatic interactions in the DSE involving K12, and for example D8, are energetically linked to the formation of transient hydrophobic clusters in the DSE. Mutation of D8 has been shown to modulate the DSE, consistent with this hypothesis (24). K12 and D8 do not interact in the native state. The two side chains project in different directions and the shortest distance between the ε-nitrogen of K12 and the carboxylate of D8 is 14.8 Å; the K12 mutation does not perturb the native state pK_a of D8 (Table S4). Our model provides another testable prediction: weakening the hydrophobic clusters should diminish the apparent coupling between K12 and other residues in the DSE.

A set of three triple mutants was prepared to compare the strength of the coupled interactions in the context of two different backgrounds that modulate DSE hydrophobic clusters. We used wild-type and hydrophobic core mutants as the backgrounds, and measured the apparent coupling between K12 and other hydrophobic sites. If K12 is energetically linked to hydrophobic clusters in the DSE, then the measured coupling free energies should be weaker in hydrophobic core mutant backgrounds that reduce these interactions. This is exactly what we observed. The analysis shows that the strong coupling observed in wild-type NTL9 is abolished or weakened significantly in all of the mutant backgrounds (I4A, A22G, L35A, A36G, A42G, and L47A) (Table S5 and Fig. 4). The coupling free energies between a given pair of residues were found to be strongly dependent upon the choice of background, with differences ranging up to as large as 1.68 kcal mol^{-1}, for residues A22 and L47. The differences are significant and are larger than or comparable to the measured coupling free energies (Table S5 and Fig. 4).

Our model makes an additional prediction: disruption of the nonnative K12 DSE interactions should alter DSE interactions that involve other residues. The data for the sets of triple mutants can be reanalyzed to obtain apparent coupling free energies between two hydrophobic residues in the wild-type and K12M backgrounds. This produces a second test of the presence of DSE interactions because the structure, dynamics, and pK_a values of the native state of the two proteins are identical. Any significant difference in the interaction free energy for a pair of residues in these two backgrounds is thus, at least in part, attributed to changes in their DSEs.

We measured the strength of the coupling interactions between three sets of residues (A22–L47, A36–A42, I4–L35) which are, respectively, 19.8, 15.2, and 12.9 Å away from each other in the native structure (Fig. S3). The coupling free energy between A22 and L47 measured in the wild-type background is −0.43 ± 0.22 kcal mol^{-1}, but is 1.25 ± 0.53 kcal mol^{-1} in the K12M background (Fig. S3). We also compared the coupling free energy of A36 and A42 in the two proteins. No coupling is observed in the wild-type background (−0.10 ± 0.22 kcal mol^{-1}), but there is a 1.05 ± 0.45-kcal mol^{-1} coupling interaction in the K12M background (Fig. S3). The coupling free energy for I4 and L35 is 0.21 ± 0.44 kcal mol^{-1} in the wild-type background and 1.65 ± 0.35 kcal mol^{-1} in the K12M background. The changes in the coupling free energies between the different backgrounds are large, and are significantly greater than the experimental uncertainty. These significant differences are fully consistent with the hypothesis that the DSE of the wild type is different from the DSE of K12M NTL9.

The m values of the mutants are similar to the wild-type value (Table S1). This may appear surprising because mutations that impact the DSE often alter m values; however, not all mutations

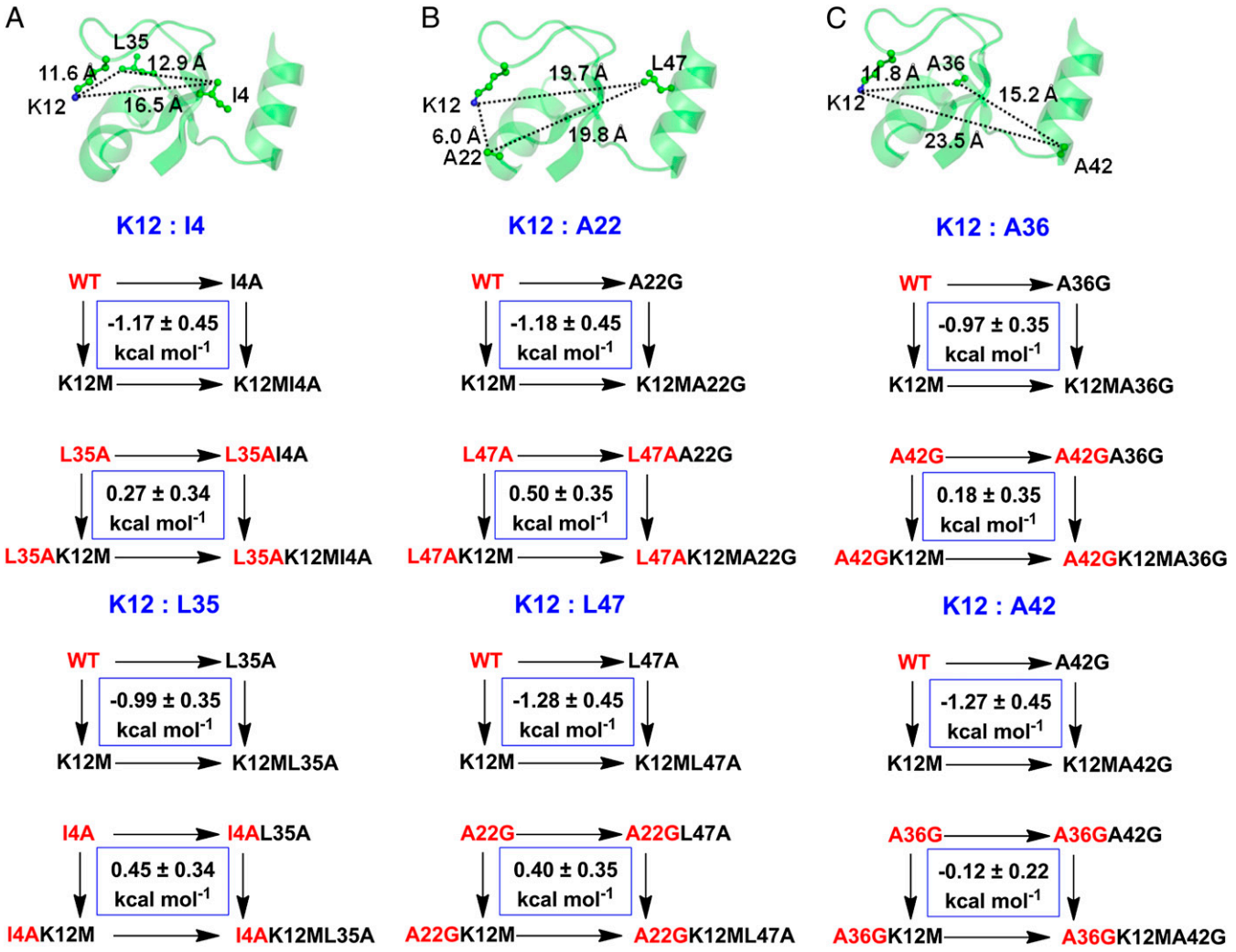

Fig. 4. Double-mutant cycle analysis reveals significant coupling in the DSE which is modulated by mutation. Couplings are large in the wild type, but are significantly reduced in mutants which weaken DSE hydrophobic clustering. (*A*) I4 and K12 measured in wild-type and in the L35A backgrounds, (*B*) A22 and K12 measured in wild-type and in the L47A backgrounds, and (C) A36 and K12 measured in wild-type and the A42G backgrounds. The data can be reanalyzed to provide the couplings between K12 and L35 in the wild-type and the I4A backgrounds, between K12 and L47 in the wild-type and the A22G backgrounds, and between K12 and A42 in the wild-type and the A36G backgrounds.

that affect the DSE lead to detectable changes in m values (36–39). In addition, the NTL9 m value is small because the protein is small and because it was measured using urea denaturation. As a consequence, even a significant relative change of the difference in solvent accessible surface area (ΔASA) between the native and DSE leads to a small change in m. A 25% change in ΔASA is predicted to lead to only a 0.08-kcal^{-1}·mol^{-1}per mol change in m for NTL9 (40). Urea m values are also believed to be more sensitive to changes in the buried amide surface area than to changes in the buried surface area of hydrocarbon. This likely contributes to the effects seen here because the mutations impact hydrophobic clusters and have less effect on residual secondary structure in the DSE (41). The major element of partially formed secondary structure in the DSE of NTL9 is the C-terminal helix, which can form in isolation in the absence of longer range contacts (42).

pH-Dependent Studies Confirm That Denatured State Ensemble Electrostatic Interactions and Hydrophobic Cluster Formation Are Linked. The K12 DSE electrostatic interactions should be reduced at low pH because K12's interaction partners will be protonated. Our model predicts that this will reduce the coupling between K12 and the hydrophobic residues in the DSE. To test this hypothesis, we measured the coupling between K12 and A22 as a function of pH from pH 6 to pH 2 (Fig. 5*A*). The wild type and mutants are fully folded over this pH range (Fig. 5*B*). The coupling is much weaker at low pH even though K12 does not titrate over this pH range and even though the K12M mutation does not affect the native state pK_as of the acidic residues. The pH-dependent effects are due to titration of the acidic residues in the DSE. At low pH the acidic residues are protonated in the DSE, which abolishes their favorable electrostatic interactions with K12. Loss of these interactions in turn weakens the measured coupling between A22 and K12. This experiment shows that the network of long-range interactions between K12 and the hydrophobic residues in NTL9 is mediated, at least in part, by DSE electrostatic interactions involving K12 and the acidic residues.

Conclusions

The pH-dependent experiments, structural and dynamic studies, and the analysis of 24 sets of double-mutant cycles show that K12 is thermodynamically coupled with hydrophobic clusters in the DSE. The analysis shows that energetically significant coupled interactions can be present in the DSE of globular proteins and

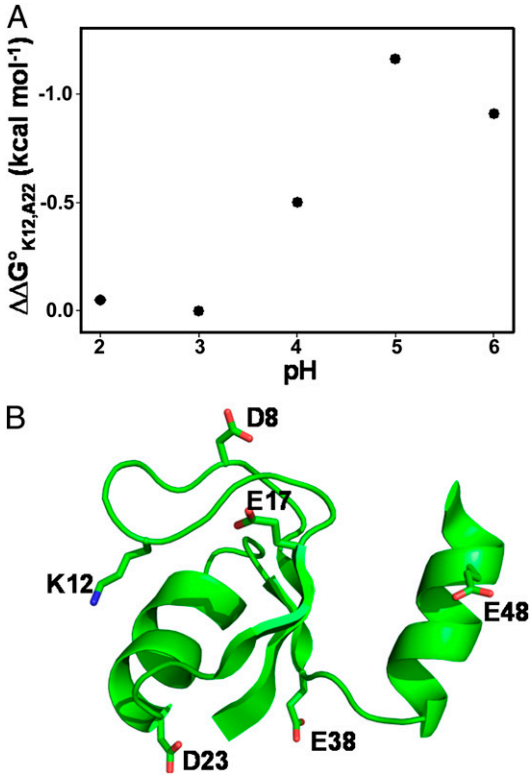

Fig. 5. pH-dependent stability studies confirm that K12 is coupled to hydrophobic residues in the DSE. (*A*) pH-dependent changes in the measured coupling free energy between K12 and A22 as determined by double-mutant cycle analysis. The coupling is abolished at low pH even though K12 does not titrate over this pH range, and even though both proteins remain fully folded over this pH range. The estimated propagated uncertainty is ± 0.45 kcal mol^{-1}. (*B*) Ribbon diagram showing the location of K12 and the acidic residues in the native structure of NTL9.

can be altered by mutation, an observation that is at odds with more traditional views of the DSE. These studies complement investigations which have demonstrated that mutations can alter the structural and dynamic properties of unfolded states by illustrating that mutations can also significantly impact DSE energetics and modulate coupled interactions in the DSE. The interactions studied here almost certainly involve residues which are well separated in primary sequence, and thus extend observations on the impact of altering local- and midrange interactions in the DSE (38, 43).

The present study illustrates how DSE effects can complicate double-mutant cycle studies, and impact the analysis of native state coupling networks; DSE effects could even lead to misleading conclusions about long-range coupling interactions in the native state. For the mutations examined here, a double-mutant cycle analysis that ignores DSE effects would lead to the conclusion that there was significant long-range coupling in the native state between K12 and a large number of hydrophobic residues, and would fail to reveal the contribution of the DSE.

Modulation of DSE interactions can also impact the analysis of protein folding by impacting Φ-values. The Φ-value is defined as the ratio of the change in the transition state free energy upon mutation relative to the change in equilibrium stability:

$$\Phi = \frac{\Delta\Delta G^{TS}}{\Delta\Delta G^{0}}. \qquad [1]$$

Φ-values have a powerful structural interpretation if the mutation does not alter DSE energetics. In this case, they report the development of interactions in the transition state and, for native interactions, represent the degree to which the interaction has developed. The situation is somewhat different if the mutation perturbs the energetics of the DSE ensemble, particularly if it modulates nonnative interactions. In this case a small Φ-value indicates that the nonnative interaction persists in the transition state (25). The Φ-value for the K12M mutation in NTL9 provides an example. The value measured in the wild-type domain is 0.26, indicating that the nonnative K12 DSE interactions persist, in part, in the transition state for folding (25). This is interesting in the context of recent long-time molecular dynamics simulations which suggest that native interactions dominate transition paths (44, 45). The present work together with studies of SH3 domains highlights the role nonnative interactions can play in the transition state for folding (38).

We measured the Φ-value for K12 in the 15 different mutant backgrounds used for the coupling analysis to explore how altering the DSE can impact Φ-values. We observed values ranging from 0.39 to 0.86. The changes in equilibrium unfolding free energy were large enough to ensure that each Φ-value was reliable (Fig. 6 and Table S6). A simple, unifying explanation for the wide range of values observed for this solvent-exposed surface site is that the second site mutations alter the energetics of the DSE and perturb the nonnative interactions made by K12 in the DSE.

The data reported here illustrate the importance of considering DSE effects when analyzing protein stability, thermodynamic cooperativity, native state coupling networks, and protein folding. There is growing evidence that the DSE can be compact under native conditions and can form native and nonnative clusters of hydrophobic residues, native and nonnative secondary structure, and even nonnative electrostatic interactions, thus the NTL9 is unlikely to be a special case (10, 12, 14, 18, 22, 27, 46, 47). NTL9 is emerging as a popular system for long molecular dynamics simulations and the data presented here will help provide a rigorous benchmark for these efforts (45, 48–50).

Methods

Protein expression and purification were performed as described previously (21). Protein stability was measured by urea chemical denaturation as described previously (21). Unfolding was monitored using the CD signal at 222 nm.

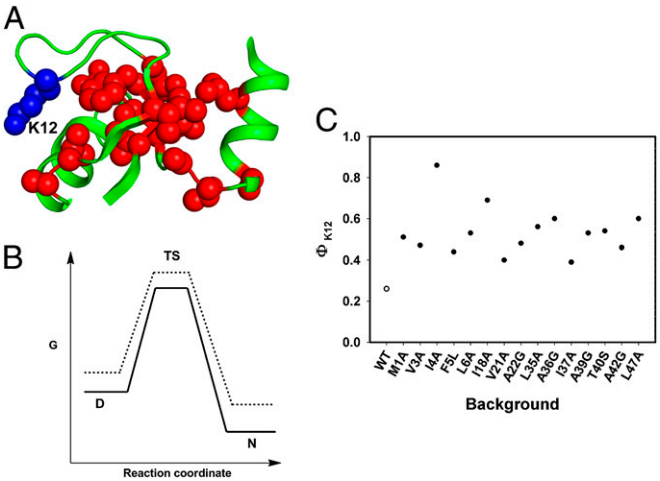

Fig. 6. Modulation of DSE energetic impacts the K12M Φ-value. (*A*) Ribbon diagram of NTL9, K12 is shown in blue and the core mutants used to generate the different backgrounds are shown in red. (*B*) Simple diagram showing the general case where a mutation (dashed lines) alters the free energy of the DSE, the transition state, and the native state. (*C*) Scatter plot of the K12 Φ-values measured in the wild type (open dot) and in different second site mutant backgrounds (black dot). The *x* axis indicates the background used.

Crystallography. Crystals were obtained at 25 °C by the hanging-drop vapor diffusion method. Diffraction data for wild-type and the K12M mutant of NTL9 were collected at the National Synchrotron Light Source at Brookhaven National Laboratory at a wavelength of 1.1 and 1.0 Å, respectively. The structure of the K12M mutant was solved (Table S3) by single isomorphous replacement with anomalous scattering. The structure of wild-type NTL9 was solved by molecular replacement using the K12M mutant as a search model. The conformation of the five C-terminal residues in the wild-type protein could not be determined due to a lack of electron density, indicating that these residues are likely flexible. In the K12M mutant the chain could be extended by one residue; however, the B factors for this residue and adjacent residues were very high. The structures have been deposited in the Protein Data Bank (PDB), ID codes 2HBB and 2HBA for NTL9 wild type and K12M NTL9, respectively. Details of crystallization and data collection are given in *SI Methods*.

NMR Spectroscopy. Two-dimensional (^{1}H, ^{1}H)-total correlation spectroscopy was measured using a Varian Inova 600-MHz spectrometer. Proton chemical shifts were referenced using trimethylsilyl propionate. The temperature coefficients of ^{1}HN chemical shifts were measured using a set of 2D ^{1}H-^{15}N heteronuclear single quantum correlation spectra recorded at various temperatures from 279.15 to 303.15 K on a Varian Inova 500 NMR spectrometer. pK_a values were determined by monitoring chemical shifts as a function of pH. ^{15}N R_1, R_2, and {^{1}H}^{15}*N*-NOE experiments were collected on a Varian 500-MHz spectrometer with a cryogenic probe for ^{15}*N*-labeled wild-type NTL9 and the K12M mutant at 25 °C .Order parameters were calculated using the Modelfree (51) approach. Details of NMR data collection and processing are given in *SI Methods*.

ACKNOWLEDGMENTS. This work was supported by National Science Foundation Grant MCB-1330259 (to D.P.R.).

1. Dyson HJ, Wright PE (2005) Intrinsically unstructured proteins and their functions. *Nat Rev Mol Cell Biol* 6(3):197–208.
2. Dobson CM (2003) Protein folding and misfolding. *Nature* 426(6968):884–890.
3. Mittag T, Forman-Kay JD (2007) Atomic-level characterization of disordered protein ensembles. *Curr Opin Struct Biol* 17(1):3–14.
4. Shortle D (1996) The denatured state (the other half of the folding equation) and its role in protein stability. *FASEB J* 10(1):27–34.
5. Baldwin RL (2002) A new perspective on unfolded proteins. *Adv Protein Chem* 62: 361–367.
6. Jahn TR, Radford SE (2008) Folding versus aggregation: Polypeptide conformations on competing pathways. *Arch Biochem Biophys* 469(1):100–117.
7. Cho JH, Sato S, Horng JC, Anil B, Raleigh DP (2008) Electrostatic interactions in the denatured state ensemble: Their effect upon protein folding and protein stability. *Arch Biochem Biophys* 469(1):20–28.
8. Bernadó P, et al. (2005) A structural model for unfolded proteins from residual dipolar couplings and small-angle x-ray scattering. *Proc Natl Acad Sci USA* 102(47): 17002–17007.
9. Hofmann H, et al. (2012) Polymer scaling laws of unfolded and intrinsically disordered proteins quantified with single-molecule spectroscopy. *Proc Natl Acad Sci USA* 109(40):16155–16160.
10. Kristjansdottir S, et al. (2005) Formation of native and non-native interactions in ensembles of denatured ACBP molecules from paramagnetic relaxation enhancement studies. *J Mol Biol* 347(5):1053–1062.
11. Ziv G, Thirumalai D, Haran G (2009) Collapse transition in proteins. *Phys Chem Chem Phys* 11(1):83–93.
12. Pashley CL, et al. (2012) Conformational properties of the unfolded state of Im7 in nondenaturing conditions. *J Mol Biol* 416(2):300–318.
13. Silvers R, et al. (2012) Modulation of structure and dynamics by disulfide bond formation in unfolded states. *J Am Chem Soc* 134(15):6846–6854.
14. Voelz VA, et al. (2012) Slow unfolded-state structuring in Acyl-CoA binding protein folding revealed by simulation and experiment. *J Am Chem Soc* 134(30):12565–12577.
15. Neri D, Billeter M, Wider G, Wüthrich K (1992) NMR determination of residual structure in a urea-denatured protein, the 434-repressor. *Science* 257(5076):1559–1563.
16. Shortle D, Ackerman MS (2001) Persistence of native-like topology in a denatured protein in 8 M urea. *Science* 293(5529):487–489.
17. Religa TL, Markson JS, Mayor U, Freund SM, Fersht AR (2005) Solution structure of a protein denatured state and folding intermediate. *Nature* 437(7061):1053–1056.
18. Klein-Seetharaman J, et al. (2002) Long-range interactions within a nonnative protein. *Science* 295(5560):1719–1722.
19. Scaloni F, Federici L, Brunori M, Gianni S (2010) Deciphering the folding transition state structure and denatured state properties of nucleophosmin C-terminal domain. *Proc Natl Acad Sci USA* 107(12):5447–5452.
20. Mok KH, et al. (2007) A pre-existing hydrophobic collapse in the unfolded state of an ultrafast folding protein. *Nature* 447(7140):106–109.
21. Cho JH, Sato S, Raleigh DP (2004) Thermodynamics and kinetics of non-native interactions in protein folding: A single point mutant significantly stabilizes the N-terminal domain of L9 by modulating non-native interactions in the denatured state. *J Mol Biol* 338(4):827–837.
22. Mok YK, Kay CM, Kay LE, Forman-Kay J (1999) NOE data demonstrating a compact unfolded state for an SH3 domain under non-denaturing conditions. *J Mol Biol* 289(3):619–638.
23. Kuhlman B, Luisi DL, Evans PA, Raleigh DP (1998) Global analysis of the effects of temperature and denaturant on the folding and unfolding kinetics of the N-terminal domain of the protein L9. *J Mol Biol* 284(5):1661–1670.
24. Cho JH, Raleigh DP (2005) Mutational analysis demonstrates that specific electrostatic interactions can play a key role in the denatured state ensemble of proteins. *J Mol Biol* 353(1):174–185.
25. Cho JH, Raleigh DP (2006) Electrostatic interactions in the denatured state and in the transition state for protein folding: Effects of denatured state interactions on the analysis of transition state structure. *J Mol Biol* 359(5):1437–1446.
26. Kuhlman B, Raleigh DP (1998) Global analysis of the thermal and chemical denaturation of the N-terminal domain of the ribosomal protein L9 in H2O and D2O. Determination of the thermodynamic parameters, deltaH(o), deltaS(o), and deltaC(o)p and evaluation of solvent isotope effects. *Protein Sci* 7(11):2405–2412.
27. Trefethen JM, Pace CN, Scholtz JM, Brems DN (2005) Charge-charge interactions in the denatured state influence the folding kinetics of ribonuclease Sa. *Protein Sci* 14(7):1934–1938.
28. Horovitz A (1996) Double-mutant cycles: A powerful tool for analyzing protein structure and function. *Fold Des* 1(6):R121–R126.
29. Horovitz A, Serrano L, Avron B, Bycroft M, Fersht AR (1990) Strength and co-operativity of contributions of surface salt bridges to protein stability. *J Mol Biol* 216(4): 1031–1044.
30. Fersht AR (1999) *Structure and Mechanism in Protein Science* (Freedman, New York).
31. Horovitz A, Fersht AR (1990) Strategy for analysing the co-operativity of intramolecular interactions in peptides and proteins. *J Mol Biol* 214(3):613–617.
32. Lin T-Y, Kim PS (1991) Evaluating the effects of a single amino acid substitution on both the native and denatured states of a protein. *Proc Natl Acad Sci USA* 88(23): 10573–10577.
33. Jain RK, Ranganathan R (2004) Local complexity of amino acid interactions in a protein core. *Proc Natl Acad Sci USA* 101(1):111–116.
34. Cierpicki T, Otlewski J (2001) Amide proton temperature coefficients as hydrogen bond indicators in proteins. *J Biomol NMR* 21(3):249–261.
35. Castañeda CA, et al. (2009) Molecular determinants of the pKa values of Asp and Glu residues in staphylococcal nuclease. *Proteins* 77(3):570–588.
36. Sánchez IE, Kiefhaber T (2003) Hammond behavior versus ground state effects in protein folding: Evidence for narrow free energy barriers and residual structure in unfolded states. *J Mol Biol* 327(4):867–884.
37. Guzman-Casado M, Parody-Morreale A, Robic S, Marqusee S, Sanchez-Ruiz JM (2003) Energetic evidence for formation of a pH-dependent hydrophobic cluster in the denatured state of Thermus thermophilus ribonuclease H. *J Mol Biol* 329(4):731–743.
38. Mok YK, Elisseeva EL, Davidson AR, Forman-Kay JD (2001) Dramatic stabilization of an SH3 domain by a single substitution: Roles of the folded and unfolded states. *J Mol Biol* 307(3):913–928.
39. Camarero JA, et al. (2001) Rescuing a destabilized protein fold through backbone cyclization. *J Mol Biol* 308(5):1045–1062.
40. Scholtz JM, Grimsley GR, Pace CN (2009) Solvent denaturation of proteins and interpretations of the m value. *Methods Enzymol* 466:549–565.
41. Guinn EJ, Kontur WS, Tsodikov OV, Shkel I, Record MT, Jr (2013) Probing the protein-folding mechanism using denaturant and temperature effects on rate constants. *Proc Natl Acad Sci USA* 110(42):16784–16789.
42. Luisi DL, Wu WJ, Raleigh DP (1999) Conformational analysis of a set of peptides corresponding to the entire primary sequence of the N-terminal domain of the ribosomal protein L9: Evidence for stable native-like secondary structure in the unfolded state. *J Mol Biol* 287(2):395–407.
43. Crowhurst KA, Tollinger M, Forman-Kay JD (2002) Cooperative interactions and a non-native buried Trp in the unfolded state of an SH3 domain. *J Mol Biol* 322(1): 163–178.
44. Best RB, Hummer G, Eaton WA (2013) Native contacts determine protein folding mechanisms in atomistic simulations. *Proc Natl Acad Sci USA* 110(44):17874–17879.
45. Lindorff-Larsen K, Piana S, Dror RO, Shaw DE (2011) How fast-folding proteins fold. *Science* 334(6055):517–520.
46. Whitten ST, García-Moreno E B (2000) pH dependence of stability of staphylococcal nuclease: Evidence of substantial electrostatic interactions in the denatured state. *Biochemistry* 39(46):14292–14304.
47. Oliveberg M, Arcus VL, Fersht AR (1995) pKA values of carboxyl groups in the native and denatured states of barnase: The pKA values of the denatured state are on average 0.4 units lower than those of model compounds. *Biochemistry* 34(29): 9424–9433.
48. Beauchamp KA, McGibbon R, Lin Y-S, Pande VS (2012) Simple few-state models reveal hidden complexity in protein folding. *Proc Natl Acad Sci USA* 109(44):17807–17813.
49. Bowman GR, Pande VS (2010) Protein folded states are kinetic hubs. *Proc Natl Acad Sci USA* 107(24):10890–10895.
50. Voelz VA, Bowman GR, Beauchamp K, Pande VS (2010) Molecular simulation of *ab initio* protein folding for a millisecond folder NTL9(1-39). *J Am Chem Soc* 132(5): 1526–1528.
51. Mandel AM, Akke M, Palmer AG, 3rd (1995) Backbone dynamics of Escherichia coli ribonuclease HI: Correlations with structure and function in an active enzyme. *J Mol Biol* 246(1):144–163.